Title

High Anion Conductivity and Low Water Uptake of Phosphonium Containing Diblock Copolymer Membranes

Journal

Macromolecules, 47(21)

ISSN

0024-9297

Authors

Cotanda, Pepa
Sudre, Guillaume
Modestino, Miguel A
et al.

Publication Date

2014-11-11

DOI

10.1021/ma501744w

Peer reviewed

Macromolecules

Article

pubs.acs.org/Macromolecules

High Anion Conductivity and Low Water Uptake of Phosphonium Containing Diblock Copolymer Membranes

Pepa Cotanda,[†,‡] Guillaume Sudre,[†,‡] Miguel A. Modestino,[†,‡] X. Chelsea Chen,[‡,§] and Nitash P. Balsara*[,†,‡,§,∥]

[†]Joint Center for Artificial Photosynthesis, Lawrence Berkeley National Laboratory, Berkeley, California 94720, United States

[‡]Department of Chemical and Biomolecular Engineering, University of California, Berkeley, Berkeley, California 94720, United States

[§]Materials Sciences Division and [∥]Environmental Energy Technologies Division, Lawrence Berkeley National Laboratory, Berkeley, California 94720, United States

ABSTRACT: Poly[(styrene)-*block*-((2-acryloxy)ethyltributylphosphonium bromide)] diblock copolymers (STBP) were synthesized in two steps. First, reversible addition−fragmentation chain transfer polymerization was used to synthesize the diblock copolymer precursors poly[(styrene)-*block*-(bromoethyl acrylate)] (SBEA), followed by functionalization with tributylphosphine. Copolymers with overall molecular weights ranging from 31 to 87 kg/mol were synthesized. The volume fraction of the ion-containing monomers in the copolymers was fixed at about 0.57. Self-assembly of these copolymers into ordered morphologies with tunable domain sizes was demonstrated by small-angle X-ray scattering. The effect of morphology on water uptake and bromide ion conductivity was explored in samples equilibrated in liquid water. The use of the pendant tributylphosphonium cations, which have some hydrophobic character, results in low water uptake and high anionic conductivity. The conductivity increases with increasing domain size while water uptake is unaffected by domain size.

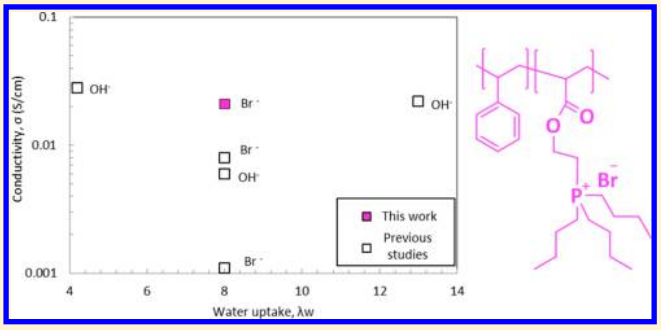

INTRODUCTION

The incorporation of ion-containing monomers into a polymer backbone generally results in a microphase-separated morphology comprising ionic and nonionic domains.[1,2] The organization of the ionic domains into continuous channels provides avenues for the transport of ions, and this is useful for a wide variety of applications such as fuel cell membranes and artificial photosynthesis.[3,4] In these applications, ion transport is facilitated by the presence of water in the ionic domains, while the mechanical integrity of the membrane is governed by the properties of both the hydrated ionic channels and the dry nonionic domains. It has been established that in dry electrolytes (e.g., lithium salts in poly(ethylene oxide), PEO) there is close coupling between segmental motion and ion transport.[5,6] Dry proton-conducting polymer electrolytes such as polystyrenesulfonate (PSS) and Nafion are nonconductive. There are many reasons for this, but slow segmental motion is certainly one contributing factor. It has also been established that in highly hydrated systems H^+ and OH^- transport occurs by the Grothuss mechanism.[7−11] We thus expect a gradual crossover from segmental motion control to Grothuss with increasing water content in hydrated polymer electrolytes. The diffusion of neutral molecules (H_2, O_2, H_2O, etc.) through the electrolyte membrane (often referred to as crossover), a factor that is detrimental to the performance of fuel cells and artificial photosynthesis devices, occurs primarily through the hydrated channels and is thus coupled to water uptake.[3,12] Block copolymers enable a systematic study of the coupling of these disparate properties.[13,14] Microphase separation in these systems is governed by structure of the monomers, block molecular weights (volume fraction), and concentration of ionic species in each block.[15,16] Ultimately, one would like to design membranes with minimum crossover of neutral molecules and optimal mechanical and electrical properties.

Most of the work in fuel cells and artificial photosynthesis is focused on acidic systems, where H^+ ions are transported between the electrodes, but the nature of the electrochemical reactions in these systems mandates the use of expensive noble metal catalysts like platinum.[17] By running these devices under alkaline conditions, where OH^- ions are transported between the electrodes, less expensive nickel-based catalysts can be used.[18−20] Anion-containing membranes are also used as biocides, water purification agents, and antistatic agents. Early work on anion-transporting membranes was focused on systems wherein quaternary ammonium or imidazolium ions were covalently bound to the polymer chain.[18,19,21] More recently, there has been significant interest in polymers with bound phosphonium ions.[22−27] Phosphonium-containing polymers often offer lower viscosity, superior conductivity in relatively dry systems, and higher thermal stability compared to

Received: August 25, 2014
Revised: October 20, 2014
Published: October 30, 2014

   dx.doi.org/10.1021/ma501744w | *Macromolecules* 2014, 47, 7540−7547

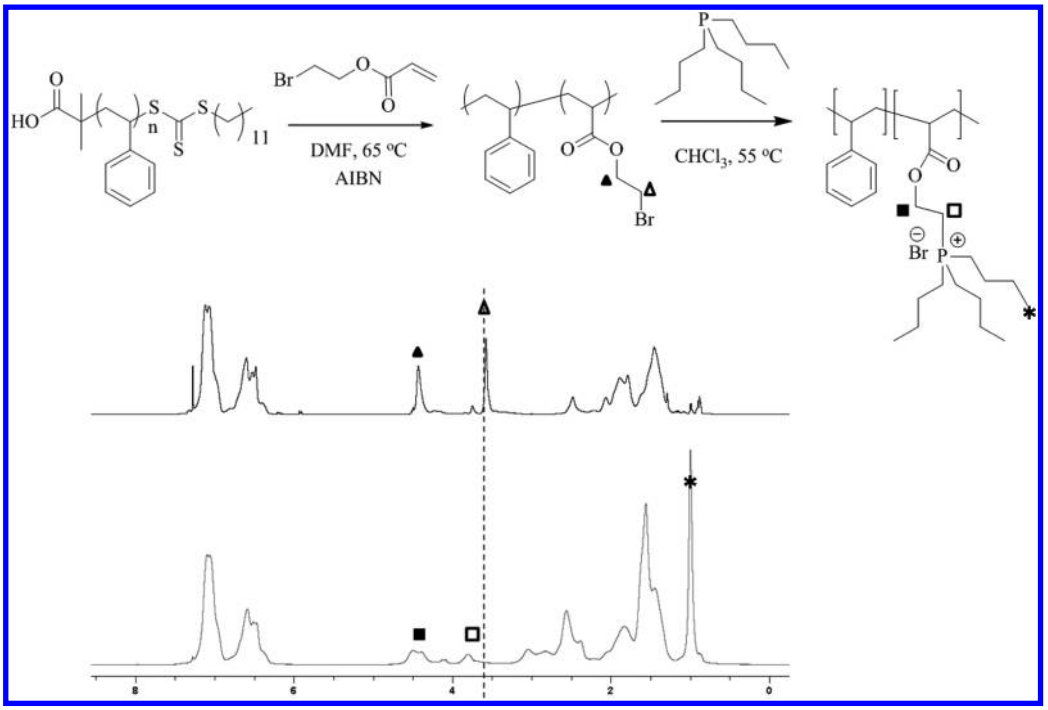

Figure 1. Synthesis of STBP polymers and ^{1}H NMR spectrum of STBP87 (bottom) and the corresponding SBEA precursor before functionalization (top).

ammonium-containing analogues.[28,29] It is well-known that, in dry systems, polymers with low T_g present higher ionic conductivities due to increased mobility of the polymer segments surrounding the ions.[30,31] Recent studies show that in hydrated systems the presence of long alkyl side chains with low T_g in the conducting block increases ionic conductivity.[15,32,33] In these studies, the increased conductivity is attributed to the formation of ion-rich channels that is facilitated by the presence of long alkyl chains. However, most of the work in anion-transporting membranes has been focused on high-T_g polymers with styrenic backbones or rigid imidazolium rings.

For all of the reasons mentioned above, the ion-containing block used in this study is based on tributylphosphonium attached to an acrylate backbone. The T_g of this polymer is relatively low (20 °C) due to the combined effect of the acrylate backbone and the presence of long alkyl chains in the phosphonium ion.[15] The hydrophobic character of the ionic polymer used in this study is expected to reduce water uptake, a key factor that controls the crossover of uncharged molecules through the membrane.[3] A similar approach was used by Li et al. to obtain hydroxide ion transporting membranes that exhibited low water uptake.[33] As the phosphonium ion is not stable under basic conditions,[24,34] this work is focused on polymers with mobile bromide ions as a model system to develop design rules for obtaining low water uptake and high conductivity in anion-conducting polymers.

A series of poly[(styrene)-*block*-(bromoethyl acrylate)] (SBEA) copolymers were synthesized by reversible addition–fragmentation chain transfer polymerization (RAFT).[35] The poly(bromoethyl acrylate) (PBEA) block was transformed into poly[(2-acryloxy)ethyltributylphosphonium bromide] (PTBP) by reaction with tributylphosphine. The overall molecular weights of the of poly[(styrene)-*block*-(tributyl bromide ethylphosphonium acrylate)] (STBP) copolymers ranged from 31 to 87 kg/mol. The volume fraction of the ion-containing monomers in the STBP copolymers was constant (or nearly so) at 0.57 ± 0.02. Our use of RAFT enables precise control over the molecular weight of each block which, in turn, controls the width of the ion-conducting domains. To our knowledge, this is the first systematic study of the effect of molecular weight on anion transport in block copolymers while keeping the volume fraction of the conducting phase more or less constant.

EXPERIMENTAL SECTION

Materials. Styrene monomer (Sigma-Aldrich) was filtered through a plug of aluminum oxide prior to use and stored at 4 °C. 2,2′-Azobis(isobutyronitrile) (AIBN, Sigma-Aldrich) was recrystallized from methanol and stored at 4 °C. All other materials were used as received from Sigma-Aldrich.

Polymer Synthesis. Polymerization of Styrene. Styrene was polymerized using previously reported procedures.[36] Styrene (500, 300, 250, and 200 equiv) and *S*-dodecyl-*S*′-(α,α′-dimethyl-α″-acetic acid)trithiocarbonate (DDMAT, 1 equiv) were introduced in an ampule. The dissolved oxygen was removed by three freeze–pump–thaw evacuation cycles. For the last cycle, nitrogen was flushed into the ampule before thawing. The ampule was put into a preheated oil bath at 110 °C. Aliquots were taken at different times and examined by ^{1}H NMR spectroscopy to determine the conversion. The polymer was precipitated twice into a stirred solution of cold methanol, filtered, and placed in a vacuum oven overnight at 40 °C. Molecular weights and dispersities were measured by gel permeation chromatography (GPC) in dimethylformamide (DMF) using polystyrene standards. ^{1}H NMR ($CDCl_3$, 400 MHz, δ): 7.41–6.25 (m, Ar–H), 2.12–1.23 (m, $-CH_2-CH-$), 0.83 (t, DDMAT CH_3).

Chain Extension of Polystyrene with BEA. Bromoethyl acrylate (BEA) was synthesized as reported elsewhere (Figure 1).[37] Polystyrene (1 equiv), BEA (140, 100, 80, and 60 equiv), and AIBN (0.2 equiv) were dissolved in tetrahydrofuran (THF, 1:1 v:v) in an ampule. The dissolved oxygen was removed by three freeze–pump–thaw evacuation cycles. For the last cycle, nitrogen was flushed into the ampule before thawing. The ampule was put into a preheated oil bath at 65 °C. Aliquots were taken at different times and examined by ^{1}H

dx.doi.org/10.1021/ma501744w | *Macromolecules* 2014, 47, 7540–7547

NMR spectroscopy to determine the conversion. The polymer was precipitated twice into a stirred solution of cold hexane, filtered, and placed in a vacuum oven overnight at 40 °C. ^{1}H NMR ($CDCl_3$, 500 MHz, δ): 7.41−6.25 (m, Ar−H), 4.43 (br t, $-CH_2-CH_2-$), 3.58 (br t, $-CH_2-CH_2-$), 2.68−1.23 (m, $-CH_2-CH-$).

Functionalization of Block Copolymers. The bromide group of the PBEA block was reacted with tributylphosphine to give the final STBP polymer as shown in Figure 1. SBEA and tributylphosphine (BEA:TBP 1:5) were dissolved in chloroform and heated at 60 °C for 2 days. The resultant polymer was precipitated in a mixture of hexane:isopropylalcohol (9:1), filtered, and dried in a vacuum oven at 40 °C overnight. Our procedure is similar to that reported by Appukuttan et al.[38] ^{1}H NMR ($CDCl_3$, 500 MHz, δ): 7.41−6.25 (m, Ar−H), 4.43 (br t, $-CH_2-CH_2-$), 3.85 (br t, $-CH_2-CH_2-$), 2.68−1.23 (m, $-CH_2-CH_2-CH_2-$), 2.68−1.23 (m, −CH2−CH−), 0.96 (t, $-CH_3$).

^{1}H Nuclear Magnetic Resonance (NMR). ^{1}H NMR spectra of the STBP diblock copolymers and the SBEA precursors were recorded with a Bruker DPX-500 spectrometer in $CDCl_3$ at 25 °C (128 scans). Typical NMR spectra obtained from these polymers are shown in Figure 1. Styrene units exhibit peaks in the 6.4−7.3 ppm range while the terminal protons on the TBP units exhibit a peak at 0.9 ppm (see Figure 1). The mole fraction of TBP (x_{TBP}) in STBP copolymers was calculated by the equation

$$x_{TBP} = \frac{\text{moles of TBP}}{\text{moles of TBP} + \text{moles of S}} = \frac{\text{integrals of peak TBP}_{0.9}/9}{\text{integrals of (peak TBP}_{0.9}/9 + \text{peak S}_{6.4-7.3}/5)}$$

Complete conversion of the bromide group in the SBEA precursor to the TBP group in the STBP polymer was confirmed by the disappearance of the NMR peak at 3.58 ppm. In addition, the mole fraction of the acrylate block in the SBEA precursor and the STBP copolymer determined by NMR were in quantitative agreement.

Gel Permeation Chromatography. Gel permeation chromatography (GPC) measurements were performed at 40 °C, using a mixture of HPLC grade dimethylformamide (DMF) and LiBr (1 g of salt per liter of DMF) as the mobile phase at a flow rate of 1 mL/min. The molecular weights of the synthesized polymers were calculated relative to polystyrene (PS) standards. Typical GPC trace of the synthesized PS and the corresponding SBEA block copolymers are shown in Figure 2. The dispersity ($Đ = M_w/M_n$) of PS precursors ranged from 1.05 to 1.13 while that of the STBP diblock copolymers ranged from 1.19 to 1.32; M_n and M_w are the number- and weight-averaged molecular weights of the samples, respectively. The higher dispersity of the diblock copolymers is probably due to side reactions that often accompany controlled radical polymerization.[39,40]

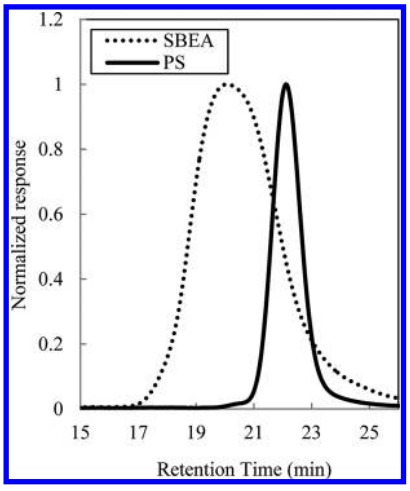

Figure 2. Refractive index signals from the DMF GPC analysis of DDMAT-terminated homopolymer and SBEA block copolymer (precursors of STBP53).

Characteristics of Polymers. Table 1 lists the diblock copolymer samples used in this study. Different samples are named as STBP followed by the nominal molecular weight of each polymer (M_n, kg/mol). Molecular weights of the PS blocks were obtained from GPC. The molecular weights of the TBP blocks were obtained by combining ^{1}H NMR spectroscopy with the measured molecular weights of the PS blocks. The volume fractions of the ion-containing blocks in STBP samples, ϕ_{TBP}, were calculated using pure component densities of PS, ρ_{PS} = 1.080 g/cm^3, and PTBP, ρ_{PTBP} = 0.898 g/cm^3, ignoring volume changes of mixing. The value of ρ_{PTBP} was measured in our laboratory by hot pressing STBP samples in a die of known volume and measuring the mass of the formed samples. Because of the presence of both charged and uncharged polymer segments, we were unable to find a solvent/column configuration that enabled GPC measurements on the STBP polymers. The dispersities of the SBEA precursors, $Đ$, were obtained by GPC and are based on PS standards.

Table 1. STBP Block Copolymers Used in This Study

polymer	M_n, STBP (kDa)	M_n, PS (kDa)	d (nm)	$Đ$	ϕ_{TBP}	x_{TBP}
STBP87	87	40	63	1.23	0.59	0.25
STBP53	53	27	46	1.32	0.55	0.22
STBP38	38	20	31	1.27	0.55	0.23
STBP31	31	14	26	1.19	0.59	0.25

Molecular weights (M_n) of the PS blocks and dispersities ($Đ = M_w/M_n$) for SBEA were obtained from GPC; molecular weights of the PBEA blocks and mole fractions of TBP (x_{TBP}) were obtained by ^{1}H NMR spectroscopy. Volume fractions (ϕ_{TBP}) calculated experimentally.

Thermogravimetric Analysis (TGA) and Differential Scanning Calorimetry (DSC). Thermogravimetric analysis (TGA) was performed on a TA TGA Q20 instrument under a nitrogen flow rate of 100 mL/min. The samples were stabilized at 100 °C and heated to 550 °C at 10 °C/min.

Differential scanning calorimetry (DSC) was performed on hot pressed membranes to determine the glass transition temperatures of the synthesized polymers using a TA DSC Q200 instrument. DSC scans consisted of three heating/cooling cycles and were conducted over the temperature range from −40 to 250 °C at a rate of 10 °C min^{-1}. For a given polymer, all cycles gave the same value of T_g.

Small-Angle X-ray Scattering. Synchrotron small-angle X-ray scattering (SAXS) measurements were performed at room temperature on 450 μm thick samples using the 7.3.3 beamline at the Advanced Light Source (ALS, Lawrence Berkeley National Laboratory).[41] Samples were prepared by hot-pressing at 155 °C for 20 min. The wavelength λ of the incident X-ray beam was 0.124 nm ($\Delta\lambda/\lambda = 10^{-4}$), and the sample-to-detector distance was 4 m. The resulting two-dimensional scattering data were averaged azimuthally to obtain intensity versus magnitude of the scattering wave vector q ($q = 4\pi \sin(\theta/2)/\lambda$, where θ is the scattering angle). The scattering data were corrected for the detector dark current and scattering from air and Kapton windows.

Electrochemical Impedance Spectroscopy. In-plane bromide conductivity of hydrated membranes with dimensions 2 cm × 1 cm × 450 μm was measured by ac impedance spectroscopy using platinum electrodes in the standard four-probe configuration using a BekkTech sample clamp. The samples were immersed in a temperature-controlled water bath. Data were collected using 10 mV amplitude over a frequency range of 1 Hz−10 MHz. Separate experiments were conducted to ensure that the response of the sample was linear in this potential window. Samples were annealed at the temperature of interest for 24−48 h until the measured resistance did not change. Fresh samples were used to measure the conductivity at each temperature. Conductivity, σ, is given by

dx.doi.org/10.1021/ma501744w | Macromolecules 2014, 47, 7540−7547

$$\sigma = \frac{w}{rS}$$

where S is the cross-sectional area of the hydrated sample film, r is the ionic resistance of the samples as determined by the intercept of the Nyquist semicircle on the real axis (Ω), and w is the distance between the inner platinum electrodes.

Water Uptake. Polymer films with thicknesses of about 450 μm were prepared by hot-pressing. The films were then immersed in water in a sealed vial, and the vial was placed in an oven at the temperature of interest. All samples were equilibrated for 72 h at each temperature. The mass of the film was measured after removing the excess water from the sample. Fresh samples were used to measure the water uptake at each temperature. The degree of hydration, λ_w, defined as the moles of water per mole of cationic groups in the membrane, is calculated using

$$\lambda_w = \frac{[H_2O]}{[TBP]} = \frac{\text{hydrated film weight} - \text{dry film weight}}{\text{dry film weight}} \times \frac{M_{TBP} + (x_{TBP}^{-1} - 1)M_S}{M_{H_2O}}$$

where the molar masses of water, styrene, and tributylphosphonium bromide acrylate monomers are M_{H_2O} = 18.02 g/mol, M_S = 104.15 g/mol, and M_{TBP} = 381.33 g/mol.

RESULTS AND DISCUSSION

The thermal stability of our polymers was evaluated using TGA. Polymer samples (dried in a vacuum oven at 100 °C overnight to drive off the water) were heated from 100 to 550 °C. SBEA samples degrade in one step with onset temperatures of 300 °C. STBP polymers exhibit a two-step degradation process: degradation of the ionic species (PTBP block) begins at 220 °C, and the degradation of the remainder of the polymer occurs at 300 °C. TGA experiments were carried out on all four STBP samples, and the degradation characteristics were similar to those shown in Figure 3a for STBP53.

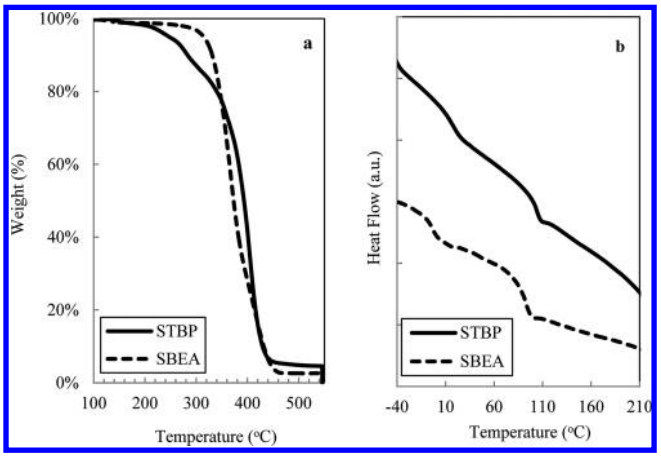

Figure 3. (a) TGA and (b) DSC of STPB53 and the SBEA precursor.

Figure 3b shows DSC results obtained from STBP53 and the corresponding SBEA precursor. STBP53 exhibited two T_gs at 20 and 102 °C. SBEA also exhibited two T_gs at −4 and 90 °C. We conclude that the measured T_g of 20 °C corresponds to the TBP-rich microphase, the T_g at −4 °C corresponds to the BEA-rich microphase, and the T_gs of 103 and 90 °C correspond to PS-rich microphases in the copolymers. The slightly lower T_g of PS chains attached to PBEA compared to that of PS chains attached to PTBP is probably due to the presence of a small concentration of PBEA chains in the PS-rich microphase.

The ionic conductivity of microphase-separated block copolymers depends on nanoscale morphology.[14,42−45] Figure 4 shows SAXS profiles obtained from STBP block copolymers

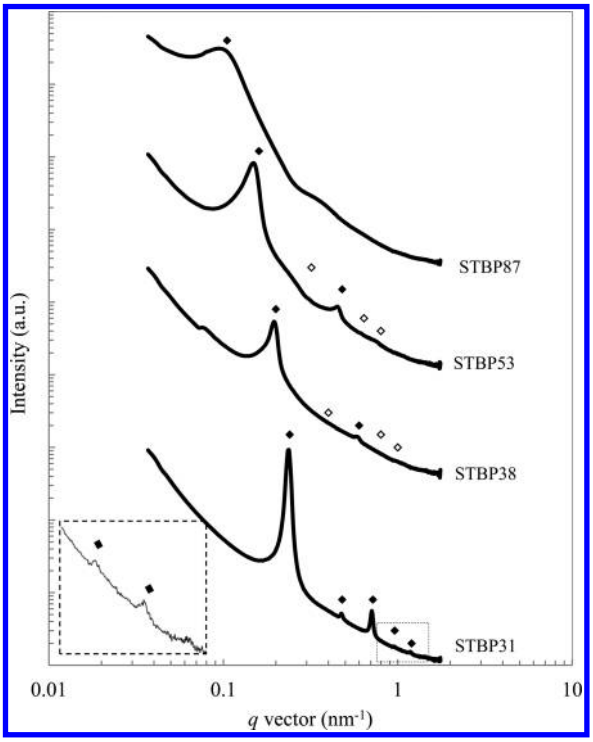

Figure 4. SAXS intensity profiles of STBP samples as a function of the magnitude of the scattering vector, q. The diamonds indicate the locations of the primary and higher order peaks at integral multiples of q^* (solid diamonds indicated existing peaks; open diamonds indicate expected peaks for lamellar structures). The scattering profiles are shifted vertically for clarity. The inset shows the SAXS profile of STBP31 on an expanded scale to clarify the locations of the fourth- and fifth-order peaks.

at 25 °C. The primary peak at $q = q^*$enables determination of the domain spacing (center-to-center distance between adjacent PS domains) $d = 2\pi/q^*$, which changes from 26 to 63 nm in our samples. In addition to the primary peak, higher order peaks are seen in most cases. In STBP31, higher order peaks are seen at $2q^*$, $3q^*$, $4q^*$, and $5q^*$. This indicates the presence of a lamellar phase. The location of the primary peak and the expected locations of higher order peaks corresponding to a lamellar phase are shown by diamonds in Figure 4. In STBP31, the second-order peak is significantly reduced in intensity relative to the third-order peak. We attribute this to the minima in the form factor of symmetric lamellae ($\phi_{TBP} \approx 0.5$, see Table 1). The second-order peaks are missing in STBP38 and STBP53 due to this effect. Missing peaks are indicated by open diamonds in Figure 4. In the case of STBP87, we obtain a broad primary peak at $q = q^*$ and a broad shoulder at higher q. The sharpness of the primary peak decreases with increasing molecular weight. We attribute this to kinetic effects: lower chain mobility of high molecular weight samples impedes the formation of lamellae with long-range order and a sharply defined d spacing.[46] The lack of higher order peaks in STBP87 precludes firm assignment of morphology. Since ϕ_{TBP} of this polymer is very similar to that of the other samples, it is likely

dx.doi.org/10.1021/ma501744w | Macromolecules 2014, 47, 7540−7547

to be lamellar. The molecular weight dependence of the SAXS profiles reported in Figure 4 is similar to that reported in the literature for other ion-containing block copolymer samples.[46]

The dependence of domain size, d, on chain length, N, of STBP polymers is shown in Figure 5. N was calculated using $N = (v_S/v_0)N_{PS} + (v_{TBP}/v_0)N_{TBP}$ based on a reference volume, v_0, of 0.1 nm^3 where the volumes of the styrene (S) and terbutylphosphonium acrylate bromide (TBP) monomers are v_S = 0.179 nm^3 and v_{TBP} = 0.424 nm^3.[47] As expected, the domain size increases with increasing N. In the case of uncharged block copolymers of a fixed composition, the domain size is predicted to be proportional to $N^{0.67}$ in the strong segregation limit.[48] A power law fit to the data in Figure 5 gives $d = 1.542 \times N^{0.86}$ nm. The exponent of N in the d versus N power law fit is a measure of chain stretching. It is evident that STBP block copolymers exhibit significantly higher chain stretching than that predicted by strong segregation theory.

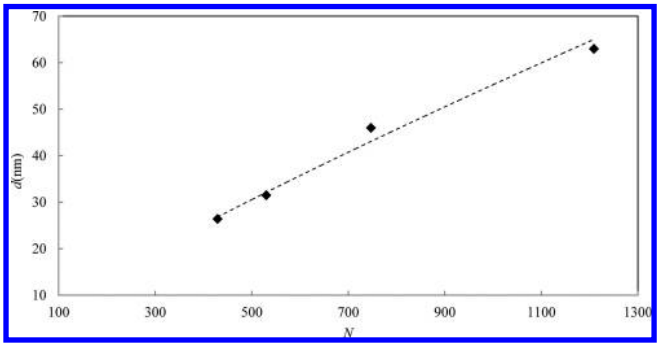

Figure 5. Variation of the domain size d of STBP block copolymer samples as a function of chain length N.

The conductivity, σ, of STBP31 immersed in water was measured as a function of increasing temperature (first run) from 21 to 71 °C (Figure 6). At each temperature, we waited until stable conductivity values were obtained (up to 72 h). Fresh samples were used to obtain conductivity at each temperature during this run. After completion of run 1, a fresh sample was heated to 71 °C and cooled in steps, and the measured conductivities obtained during this run are also shown in Figure 6 (second run). The conductivities obtained during the first run are in reasonable agreement with those obtained during the second run. The straight line in Figure 6 is the least-squares fit through the conductivity data obtained from both runs.

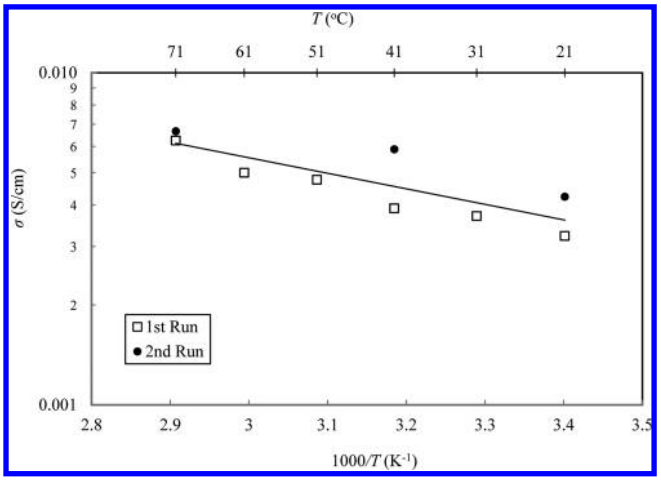

Figure 6. Conductivity as a function of inverse temperature of STBP31.

Ionic conductivity in polymer electrolyte membranes depends crucially on water content. The water uptake data of STBP87 and STBP31 samples (the polymers with largest and smallest chain length) are shown in Figure 7. To ensure equilibration, a waiting time of 72 h was used before each measurement. In both cases, the degree of hydration is not dependent on temperature or polymer molecular weight (domain spacing) from 25 to 71 °C. To a good approximation, λ_w is about 8 in the temperature range of interest. In principle, the change in conductivity with temperature reported in Figure 6 can arise due to changes in mobility of bromide ions, changes in segmental mobility of the polymer chains, or changes in ion concentration in the membrane due to differences in water uptake. The fact that water uptake in the membranes is more or less constant at $\lambda_w \approx 8$ indicates that the slope of the line in Figure 6 provides an estimate of the activation energy for transport of bromide ions through the membrane (Arrhenius law). The estimated activation energy is 9.1 kJ/mol, which is 2.5 times lower than that reported previously for the chloride conductivity of poly(styrene-*b*-4-vinylbenzyltrimethylammonium chloride) under the same conditions, 22.7 kJ/mol,[21] 3 times lower than the bromide conductivity of 1-[(2-methacryloyloxy)ethyl]-3-butylimidazolium bromide diblock copolymers at 90% RH (relative humidity), 29 kJ/mol,[49] and comparable to that for the proton conductivity of Nafion at 100% RH, 7.4 kJ/mol.[50]

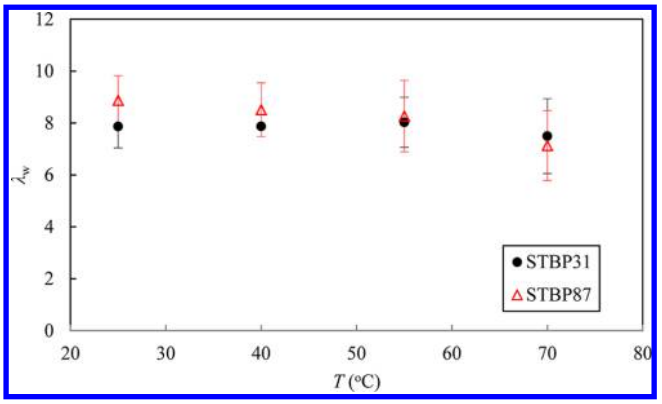

Figure 7. Water uptake λ_w (moles of water per phosphonium group) as a function of temperature of STBP31 and STBP87.

To our knowledge, the effect of domain size on anion conductivity of hydrated polymer electrolyte membranes (keeping composition and fraction of ionic groups constant) has not yet been reported. The ionic conductivity of STBP membranes at 25 °C is shown as a function of domain size in Figure 8. It is evident that increasing the domain size results in a 3-fold increase in anionic conductivity, from 0.006 S/cm for a domain size of 26 nm to 0.021 S/cm for a domain size of 63 nm. In proton-conducting hydrated block copolymer electrolyte membranes equilibrated in humid air, increasing the domain size from 23 to 80 nm results in a more modest increase in conductivity at temperatures between 25 and 60 °C.[16] Similar increases in conductivity with domain size have also been seen in mixtures of block copolymers and lithium salts.[46,51] The reason for the observed increase in conductivity in these systems has not been fully established. There are,

dx.doi.org/10.1021/ma501744w | Macromolecules 2014, 47, 7540−7547

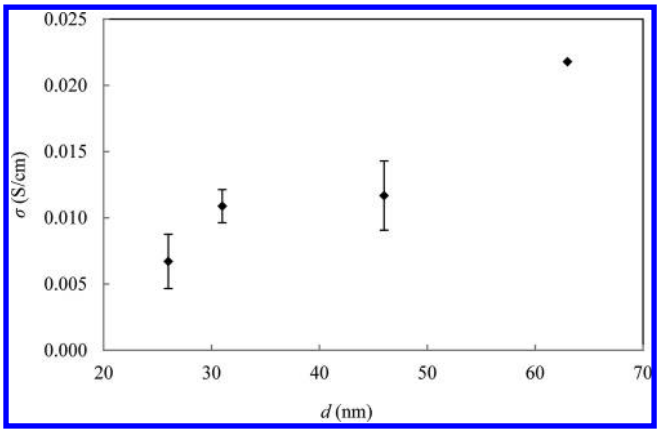

Figure 8. Room temperature ionic conductivity as a function of domain size for STBP polymers.

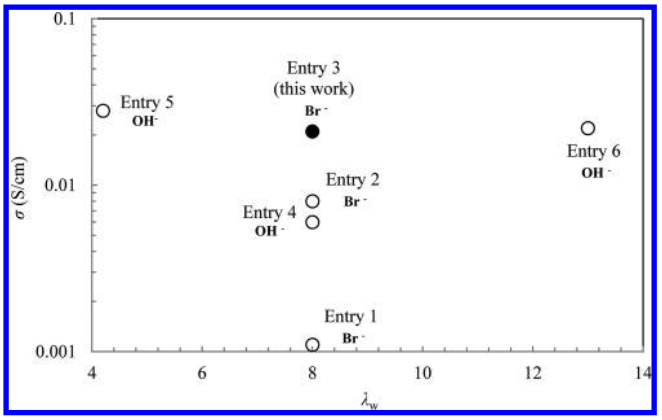

Figure 9. Values of ionic conductivity versus water uptake for different membranes. Details concerning membranes taken from the literature are given in Table 2.

however, three possible explanations for this observation: (1) Ions near the interface between the soft conducting channels and the glassy nonconducting channels may exhibit lower mobility. The fraction of such ions decreases with increasing domain size (or equivalently with increasing molecular weight).[52] (2) The stretching of polymer chains within block copolymer domains is nonuniform and depends on chain length; segments near the center of the domains are in relaxed configurations. This results in the migration of charged species toward the center of domains in mixtures of lithium salts and high molecular weight block copolymers.[53] (3) Defect annihilation in block copolymers is expected to slow down dramatically with increasing molecular weight. In mixtures of lithium salts and block copolymers, it has been established that defect annihilation lowers conductivity.[54] Further work is necessary to establish the extent to which the three effects listed above apply to anion-conducting diblock copolymers swollen with water.

We conclude this section by comparing anion conductivity of STBP87 with that reported in the literature. We focus on polymers with relatively low water uptake ($\lambda_w \leq 13$). The polymers chosen for this comparison are listed in Table 2. Figure 9 shows anion conductivity versus water uptake for all polymers listed in Table 2. Entry 1 in Table 2 is an imidazolium-based block copolymer with $\lambda_w \approx 8$ and conductivity of 0.001 S/cm reported by Ye et al. at 30 °C and 90% RH.[55] In a recent report, the same group synthesized a new low-T_g imidazolium-containing diblock copolymer with a similar value of λ_w and a significantly higher bromide ion conductivity of 0.008 S/cm at 50 °C and 90% RH.[32] Li et al. studied hydroxide ion transport in a poly(phenylene oxide) (PPO) sample containing randomly located quaternary ammonium functional groups and obtained σ = 0.006 S/cm at $\lambda_w \approx 8$ and 25 °C in liquid water.[33] In the same paper, Li et al. increased the length of the alkyl chains of the functional group and obtained σ = 0.028 S/cm at λ_w = 4.2 and 25 °C in liquid water. Hydroxide ion conductivity of 0.022 S/cm was reported by Noonan et al. for a new membrane based on a tetrakis(dialkylamino)phosphonium cation at 22 °C in liquid water.[23] However, the water uptake of this membrane was higher than that of the membranes described above (λ_w = 13). The bromide ion conductivity of STBP87 is 0.021 S/cm, very similar to that obtained by Noonan et al. for hydroxide ions, but with a reduced $\lambda_w \approx 8$. For completeness we note that the proton conductivity of Nafion for $\lambda_w \approx 8$ is 0.03 S/cm.[9] At 25 °C, the conductivity of an aqueous HBr solution with $\lambda_w \approx 8$ (7 M) is 0.78 S/cm.[56] The Br^- transference number in 7 M aqueous HBr solution at this temperature is 0.19.[57] The estimated conductivity of bromide ions alone in unconstrained aqueous solutions at 25 °C at this concentration is thus 0.15 S/cm,[56−58] a value that is much larger than the conductivity of hydrated STBP87. In aqueous environments, proton and hydroxide ion transport is much faster than that of bromide ions due to the dominance of the Grotthuss transport mechanism. It appears that employing an ion-conducting polymer with low T_g and high hydrophobicity due to the acrylate backbone and to the presence of long alkyl chains, combined with the electronic structure of the phosphonium cation, results in high bromide conductivity at low water uptake. Further work is needed to establish the quantitative relationships between water uptake and ionic conductivity and the relative importance of segmental motion on ion transport as a function of water uptake.

Table 2. Characteristics of the Membranes Reported in Figure 9

entry	polymer	λ_w	σ (S/cm)	IEC[a]	T_g (°C)	ion	T (°C)	% RH
1	PMMA-*b*-PBIm[55]	8	0.0011	1.4	110	Br	30	90
2	PMMA-*b*-PBOIm[32]	8	0.008	1.9	23	Br	50	90
3	STBP87, this work	8	0.021	1.4	20	Br	25	liquid water
4	PPO with trimethylamonium[33]	8	0.006	1.2	*b*	OH	25	liquid water
5	PPO with dimethylhexylamonium[33]	4.2	0.028	1.8	*b*	OH	25	liquid water
6	PE-*r*-[P(N(Me)Cy)$_4$][23]	13	0.022	0.9	*b*	OH	22	liquid water

[a]In mequiv ion/g polymer. [b]Unspecified.

dx.doi.org/10.1021/ma501744w | *Macromolecules* 2014, 47, 7540−7547

CONCLUSIONS

Four different poly[(styrene-*block*-(bromoethyl acrylate)] (SBEA) copolymers were synthesized by RAFT, followed by postfunctionalization with tributylphosphine to transform the PBEA block into an anion-conductive poly-(tributylphosphonium bromide acrylate) (PTBP) block. All copolymers have a similar volume fraction of functional block, about 0.57, and molecular weights from 31 to 87 kg/mol. The copolymers self-assemble to give lamellar morphologies (higher order SAXS peaks were obtained in three out of four samples), and the domain size increases with molecular weight. Bromide ion conductivities were measured for samples equilibrated in liquid water. Increasing domain size by a factor of 2 results in a 3-fold increase in conductivity. In contrast, water uptake is unaffected by the increase in domain size. STBP block copolymers exhibit low water uptake ($\lambda_w \approx 8$) and high ionic conductivity (above 10^{-3} S/cm). The low water uptake is attributed to the presence of long alkyl chains on the pendant ionic group (tributylphosphine), and high ionic conductivity is attributed to the long alkyl chains and electronic structure of the phosphonium cation. The low water content of these materials may enable the design of membranes that efficiently transport anions but prevent the crossover of neutral molecules through the water channels. Such membranes may ultimately be useful for fuel cells and artificial photosynthesis.

AUTHOR INFORMATION

Corresponding Author

*E-mail: nbalsara@berkeley.edu (N.P.B.).

Notes

The authors declare no competing financial interest.

ACKNOWLEDGMENTS

This material is based upon work performed by the Joint Center for Artificial Photosynthesis, a DOE Energy Innovation Hub, supported through the Office of Science of the U.S. Department of Energy under Award DE-SC0004993. SAXS experiments were performed at Lawrence Berkeley National Laboratory's Advance Light Source, Beamline 7.3.3. Beamline 7.3.3 of the Advanced Light Source is supported by the Director of the Office of Science, Office of Basic Energy Sciences, of the U.S. Department of Energy under Contract DE-AC02-05CH11231.

REFERENCES

(1) Gierke, T. D.; Munn, G. E.; Wilson, F. C. *J. Polym. Sci., Polym. Phys. Ed.* **1981**, *19*, 1687.
(2) Mauritz, K. A.; Moore, R. B. *Chem. Rev.* **2004**, *104*, 4535.
(3) Berger, A.; Segalman, R. A.; Newman, J. *Energy Environ. Sci.* **2014**, *7*, 1468.
(4) Elabd, Y. A.; Hickner, M. A. *Macromolecules* **2010**, *44*, 1.
(5) Kakihana, M.; Schantz, S.; Torell, L. M. *J. Chem. Phys.* **1990**, *92*, 6271.
(6) Boden, N.; Leng, S. A.; Ward, I. M. *Solid State Ionics* **1991**, *45*, 261.
(7) Zawodzinski, T. A.; Neeman, M.; Sillerud, L. O.; Gottesfeld, S. *J. Phys. Chem.* **1991**, *95*, 6040.
(8) Zawodzinski, T. A.; Davey, J.; Valerio, J.; Gottesfeld, S. *Electrochim. Acta* **1995**, *40*, 297.
(9) Zawodzinski, T. A.; Derouin, C.; Radzinski, S.; Sherman, R. J.; Smith, V. T.; Springer, T. E.; Gottesfeld, S. *J. Electrochem. Soc.* **1993**, *140*, 1041.
(10) Weber, A. Z.; Newman, J. *J. Electrochem. Soc.* **2004**, *151*, A311.
(11) Weber, A. Z.; Newman, J. *J. Electrochem. Soc.* **2003**, *150*, A1008.
(12) Hallinan, D. T.; Elabd, Y. A. *J. Phys. Chem. B* **2007**, *111*, 13221.
(13) Peckham, T. J.; Holdcroft, S. *Adv. Mater.* **2010**, *22*, 4667.
(14) Choi, J.-H.; Ye, Y.; Elabd, Y. A.; Winey, K. I. *Macromolecules* **2013**, *46*, 5290.
(15) Weber, R. L.; Ye, Y.; Banik, S. M.; Elabd, Y. A.; Hickner, M. A.; Mahanthappa, M. K. *J. Polym. Sci., Part B: Polym. Phys.* **2011**, *49*, 1287.
(16) Park, M. J.; Downing, K. H.; Jackson, A.; Gomez, E. D.; Minor, A. M.; Cookson, D.; Weber, A. Z.; Balsara, N. P. *Nano Lett.* **2007**, *7*, 3547.
(17) Hickner, M. A.; Pivovar, B. S. *Fuel Cells* **2005**, *5*, 213.
(18) Merle, G.; Wessling, M.; Nijmeijer, K. *J. Membr. Sci.* **2011**, *377*, 1.
(19) Couture, G.; Alaaeddine, A.; Boschet, F.; Ameduri, B. *Prog. Polym. Sci.* **2011**, *36*, 1521.
(20) Hickner, M. A.; Herring, A. M.; Coughlin, E. B. *J. Polym. Sci., Part B: Polym. Phys.* **2013**, *51*, 1727.
(21) Sudre, G.; Inceoglu, S.; Cotanda, P.; Balsara, N. P. *Macromolecules* **2013**, *46*, 1519.
(22) Jangu, C.; Long, T. E. *Polymer* **2014**, *16*, 3298.
(23) Noonan, K. J. T.; Hugar, K. M.; Kostalik, H. A.; Lobkovsky, E. B.; Abruña, H. D.; Coates, G. W. *J. Am. Chem. Soc.* **2012**, *134*, 18161.
(24) Ye, Y.; Stokes, K. K.; Beyer, F. L.; Elabd, Y. A. *J. Membr. Sci.* **2013**, *443*, 93.
(25) Bradaric, C. J.; Downard, A.; Kennedy, C.; Robertson, A. J.; Zhou, Y. *Green Chem.* **2003**, *5*, 143.
(26) Fraser, K. J.; MacFarlane, D. R. *Aust. J. Chem.* **2009**, *62*, 309.
(27) Gu, S.; Cai, R.; Yan, Y. *Chem. Commun.* **2011**, *47*, 2856.
(28) Hemp, S. T.; Zhang, M.; Allen, M. H.; Cheng, S.; Moore, R. B.; Long, T. E. *Macromol. Chem. Phys.* **2013**, *214*, 2099.
(29) Liang, S.; O'Reilly, M. V.; Choi, U. H.; Shiau, H.-S.; Bartels, J.; Chen, Q.; Runt, J.; Winey, K. I.; Colby, R. H. *Macromolecules* **2014**, *47*, 4428.
(30) Mecerreyes, D. *Prog. Polym. Sci.* **2011**, *36*, 1629.
(31) Choi, U. H.; Ye, Y.; Salas de la Cruz, D.; Liu, W.; Winey, K. I.; Elabd, Y. A.; Runt, J.; Colby, R. H. *Macromolecules* **2014**, *47*, 777.
(32) Nykaza, J. R.; Ye, Y.; Elabd, Y. A. *Polymer* **2014**, *55*, 3360.
(33) Li, N.; Leng, Y.; Hickner, M. A.; Wang, C.-Y. *J. Am. Chem. Soc.* **2013**, *135*, 10124.
(34) Yuesheng, Y.; Yossef, A. E. In *Polymers for Energy Storage and Delivery: Polyelectrolytes for Batteries and Fuel Cells*; American Chemical Society: Washington, DC, 2012; Vol. *1096*, p 233.
(35) Chiefari, J.; Chong, Y. K.; Ercole, F.; Krstina, J.; Jeffery, J.; Le, T. P. T.; Mayadunne, R. T. A.; Meijs, G. F.; Moad, C. L.; Moad, G.; Rizzardo, E.; Thang, S. H. *Macromolecules* **1998**, *31*, 5559.
(36) Cotanda, P.; Lu, A.; Patterson, J. P.; Petzetakis, N.; O'Reilly, R. K. *Macromolecules* **2012**, *45*, 2377.
(37) Gu, Y.; Lodge, T. P. *Macromolecules* **2011**, *44*, 1732.
(38) Appukuttan, V. K.; Dupont, A.; Denis-Quanquin, S.; Andraud, C.; Monnereau, C. *Polym. Chem.* **2012**, *3*, 2723.
(39) Moad, G.; Rizzardo, E.; Thang, S. H. *Aust. J. Chem.* **2005**, *58*, 379.
(40) Braunecker, W. A.; Matyjaszewski, K. *Prog. Polym. Sci.* **2007**, *32*, 93.
(41) Hexemer, A.; Bras, W.; Glossinger, J.; Schaible, E.; Gann, E.; Kirian, R.; MacDowell, A.; Church, M.; Rude, B.; Padmore, H. *J. Phys.: Conf. Ser.* **2010**, *247*, 012007.
(42) Schneider, Y.; Modestino, M. A.; McCulloch, B. L.; Hoarfrost, M. L.; Hess, R. W.; Segalman, R. A. *Macromolecules* **2013**, *46*, 1543.
(43) Ye, Y.; Choi, J.-H.; Winey, K. I.; Elabd, Y. A. *Macromolecules* **2012**, *45*, 7027.
(44) Weber, R. L.; Ye, Y.; Schmitt, A. L.; Banik, S. M.; Elabd, Y. A.; Mahanthappa, M. K. *Macromolecules* **2011**, *44*, 5727.
(45) Tsai, T.-H.; Maes, A. M.; Vandiver, M. A.; Versek, C.; Seifert, S.; Tuominen, M.; Liberatore, M. W.; Herring, A. M.; Coughlin, E. B. *J. Polym. Sci., Part B: Polym. Phys.* **2013**, *51*, 1751.
(46) Singh, M.; Odusanya, O.; Wilmes, G. M.; Eitouni, H. B.; Gomez, E. D.; Patel, A. J.; Chen, V. L.; Park, M. J.; Fragouli, P.; Iatrou, H.; Hadjichristidis, N.; Cookson, D.; Balsara, N. P. *Macromolecules* **2007**, *40*, 4578.

(47) Eitouni, H.; Balsara, N. In *Physical Properties of Polymers Handbook*; Mark, J., Ed.; Springer: New York, 2007; p 339.
(48) Helfand, E.; Wasserman, Z. R. *Macromolecules* **1976**, *9*, 879.
(49) Price, S. C.; Ren, X.; Jackson, A. C.; Ye, Y.; Elabd, Y. A.; Beyer, F. L. *Macromolecules* **2013**, *46*, 7332.
(50) Varcoe, J. R. *Phys. Chem. Chem. Phys.* **2007**, *9*, 1479.
(51) Panday, A.; Mullin, S.; Gomez, E. D.; Wanakule, N.; Chen, V. L.; Hexemer, A.; Pople, J.; Balsara, N. P. *Macromolecules* **2009**, *42*, 4632.
(52) Ganesan, V.; Pyramitsyn, V.; Bertoni, C.; Shah, M. *ACS Macro Lett.* **2012**, *1*, 513.
(53) Gomez, E. D.; Panday, A.; Feng, E. H.; Chen, V.; Stone, G. M.; Minor, A. M.; Kisielowski, C.; Downing, K. H.; Borodin, O.; Smith, G. D.; Balsara, N. P. *Nano Lett.* **2009**, *9*, 1212.
(54) Chintapalli, M.; Chen, X. C.; Thelen, J. L.; Teran, A. A.; Wang, X.; Garetz, B. A.; Balsara, N. P. *Macromolecules* **2014**, *47*, 5424.
(55) Ye, Y.; Sharick, S.; Davis, E. M.; Winey, K. I.; Elabd, Y. A. *ACS Macro Lett.* **2013**, *2*, 575.
(56) Hamer, W. J.; DeWane, H. J. *Electrolytic Conductance and the Conductances of the Halogen Acids in Water*; U.S. National Bureau of Standards; for sale by the Supt. of Docs.; U.S. Government Printing Office: Washington, DC, 1970.
(57) Augustynski, J. W.; Faita, G.; Mussini, T. *J. Chem. Eng. Data* **1967**, *12*, 369.
(58) Chen, X. C.; Wong, D. T.; Yakovlev, S.; Beers, K. M.; Downing, K. H.; Balsara, N. P. *Nano Lett.* **2014**, *14*, 4058.